4. F. R. Hallett and R. A. B. Keates, *ibid.*, p. 2403.
5. M. F. Carlier, T. L. Hill, Y. D. Chen, *Proc. Natl. Acad. Sci. U.S.A.* **81**, 771 (1984).
6. Y. D. Chen and T. L. Hill, *ibid.* **82**, 1131 (1985).
7. D. Kristofferson, T. J. Mitchison, M. W. Kirschner, *J. Cell Biol.* **102**, 1007 (1986).
8. T. Horio and H. Hotani, *Nature* **321**, 605 (1986).
9. Microtubule protein, prepared in a mixture of 0.1*M* MES K^+ (the potassium salt of 4-morpholineethanesulfonic acid), 2 m*M* magnesium acetate, and 1 m*M* EGTA buffer, *p*H 6.6 (MME) [R. A. B. Keates, *Can. J. Biochem. Cell Biol.* **62**, 803 (1984)], was estimated to contain 25% MAPs and 74% tubulin by scanning densitometry. We then added NaCl and glycerol to attain concentrations of 0.3*M* and 2*M*, respectively, and the solution was applied to a DEAE-Sepharose CL-6B column (1.5 cm by 8 cm). MAPs were eluted with 0.3*M* NaCl, 2*M* glycerol in MME. MAP-free tubulin was eluted with 0.5*M* NaCl, 2*M* glycerol in MME, and was dialyzed overnight against 5*M* glycerol in MME. We observed that the purified tubulin self-assembled into microtubules after increasing $[Mg^{2+}]$ to 5 m*M*, adding GTP to 1 m*M*, and raising the temperature to 37°C. One cycle of assembly and disassembly after the column step enriched for polymerization-active protein.
10. The sample (prepared and incubated as in Fig. 3A) was illuminated by a HeNe laser (15 mW, 632.8 nm) and was monitored at 90° to the incident beam. Intensity fluctuations detected by a quantum photometer (model 1140, Princeton Applied Research, Princeton, NJ) were correlated with a digital autocorrelator (model 1096, Langley-Ford Instruments, Amherst, MA). The resulting intensity autocorrelation functions were analyzed with a long-rod approximation developed specifically for systems such as microtubules (*3*). We determined microtubule lengths by using the exponential sampling method of Hallett and Keates (*4*), except that a nonnegative least squares routine [I. D. Morrison, E. F. Grabowsky, C. A. Herb, *Langmuir* **1**, 496 (1985)] was included in the fitting procedure. QELS-derived distributions have been verified with microtubule samples measured by electron microscopy (*4*). Typical length distributions were broad and highly skewed; a sample with a mean length of 16 μm contained components from 1 to over 60 μm.
11. R. A. Walker *et al.*, *J. Cell Biol.* **105**, 29a (1987).
12. S. W. Rothwell, W. A. Grasser, H. N. Baker, D. B. Murphy, *ibid.*, p. 863; M. Caplow, J. Shanks, B. P. Brylawski, *J. Biol. Chem.* **261**, 16233 (1986).
13. E. Schulze and M. W. Kirschner, *J. Cell Biol.* **104**, 277 (1987).
14. P. J. Sammak *et al.*, *ibid.*, p. 395.
15. We thank J. Marsh and C. Samuels for technical assistance. This work was supported by grants from the Natural Sciences and Engineering Research Council of Canada.

16 February 1988; accepted 13 July 1988

Accelerated Electron Transfer Between Metal Complexes Mediated by DNA

MICHAEL D. PURUGGANAN, CHALLA V. KUMAR, NICHOLAS J. TURRO,* JACQUELINE K. BARTON*

DNA-mediated long-range electron transfer from photoexcited 1,10-phenanthroline complexes of ruthenium, $Ru(phen)_3^{2+}$, to isostructural complexes of cobalt(III), rhodium(III), and chromium(III) bound along the helical strand. The efficiency of transfer depended upon binding mode and driving force. For a given donor-acceptor pair, surface-bound complexes showed greater rate enhancements than those that were intercalatively bound. Even in rigid glycerol at 253 K, the rates for donor-acceptor pairs bound to DNA remained enhanced. For the series of acceptors, the greatest enhancement in electron-transfer rate was found with chromium, the acceptor of intermediate driving force. The DNA polymer appears to provide an efficient intervening medium to couple donor and acceptor metal complexes for electron transfer.

AN UNDERSTANDING OF HOW ELECtrons are transferred over large distances is essential to the characterization of fundamental redox processes in biology such as oxidative phosphorylation and photosynthesis (*1*). The study of long-range electron transfer also contributes significantly to our ability to construct efficient molecular assemblies that can carry out electrochemical reactions. Studies of electron transfer between excited zinc porphyrins and heme centers in protein-protein complexes and between solvent accessible residues modified with pentammine ruthenium and the interior of structurally characterized metalloproteins have shown that electron transfer can occur over large distances through protein interiors (*2, 3*). Theory indicates that such factors as donor-acceptor distance, thermodynamic driving force, and the nature of the intervening medium are critical in determining rates of electron transfer (*4, 5*). Model compounds with variable exothermicity and distance between donor-acceptor pairs have been synthesized, and the rates of intramolecular electron transfer in these provide benchmarks for studies in more complex polymeric systems (*6, 7*).

We report that the double-stranded DNA polymer may also mediate long-range electron transfer between bound donor-acceptor pairs. The apparent enhancement in photoinduced electron-transfer rates for donor-acceptor pairs bound to DNA versus being free in solution is several orders of magnitude (*8, 9*). This apparent rate enhancement in the presence of DNA could be attributed to (i) the increase in local concentration of bound donor-acceptor pairs, (ii) facilitated diffusion of the bound pair along the DNA helix in a reduced dimensional space, and (iii) long-range electron transfer between donor and acceptor pairs with DNA as the intervening medium. By varying temperature, viscosity, and driving force, we show that DNA-mediated electron transfer from $Ru(phen)_3^{2+}$ to $M(phen)_3^{3+}$, where M = Rh, Cr, or Co, may occur, at least in part, through long-range electron transfer.

A current model for the interaction of tris(phenanthroline) metal complexes with DNA is shown in Fig. 1. The rigid metal complex, $Ru(phen)_3^{2+}$, appears to bind to double-stranded DNA primarily through two distinct modes: (i) intercalation, in which one of the phenanthroline ligands may insert and stack in between the base pairs, and (ii) surface or groove binding, in which the hydrophobicity of the phenanthroline ligands as well as the electrostatic charge of the ruthenium dication stabilize binding against the helical groove of the DNA polyanion (*10, 11*). These binding modes have been characterized primarily through photophysical experiments, such as the differential quenching of two types of ruthenium excited states by anionic quenchers, the retention of polarized emission for the intercalative component when excited with polarized light, and the observation of two distinct lifetimes, 0.6 and 2.0 μs, for the surface-bound and intercalated ruthenium

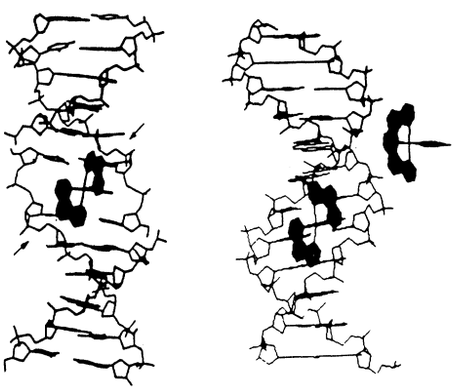

Fig. 1. Model for $Ru(phen)_3^{2+}$ bound to a B-DNA helix, showing (left) intercalation of the Δ-isomer and (right) the surface-binding of the Λ-isomer. For intercalated Δ-$Ru(phen)_3^{2+}$, the intercalated ligand is shown pointed into the page. The arrows indicate the alignment of the non-intercalated ligands along the right-handed helical groove. For the surface-bound Λ isomers, a side view (top) and front view (bottom, with the third ligand pointing out of the page) are shown.

Department of Chemistry, Columbia University, New York, NY 10027.

*To whom correspondence should be addressed.

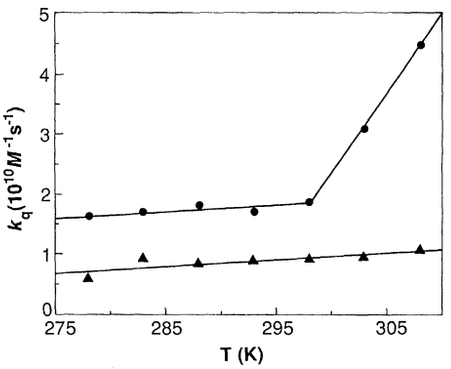

Fig. 2. Temperature dependence of the electron-transfer rate constants between (●) surface and (▲) intercalated DNA-bound donors and acceptors. The donor is Δ-Ru(phen)$_3^{2+*}$ and the acceptor is *rac*-Co(phen)$_3^{3+}$. Solution concentrations were as those described in Table 1. Lifetime measurements were made at least in triplicate.

excited states, respectively. Nuclear magnetic resonance and photophysical studies suggest that surface binding occurs from the minor groove of DNA, whereas intercalation of the complexes proceeds from the major groove. Although both enantiomers of the metal complexes bind to the helix through the two modes, opposite chiral selectivity is observed with these different binding modes. The right-handed propeller-like Δ-isomer intercalates preferentially into the right-handed B-DNA helix because of the reduced steric constraints between its nonintercalated ligands and the phosphate backbone, whereas for surface binding, where the complex lies against the right-handed helix, the Λ-isomer, which has a symmetry that complements that of the helix, is favored (*12*). The differing enantiomeric selectivities and the different excited state lifetimes for the two binding modes allow us to probe the effect of donor binding mode on electron transfer, since the photoinduced electron-transfer rate constants for the two modes may be separately determined in a time-resolved luminescence-quenching experiment by using DNA-bound cobalt, chromium, or rhodium complexes as electron acceptors.

Emission decays were determined for the ruthenium complexes by single-photon counting with a nanosecond flash lamp (full width at half maximum of 3 ns) as a function of titration with the electron acceptors M(phen)$_3^{3+}$ (M = Rh, Cr, and Co) and Co(bpy)$_3^{3+}$ (bpy = 2,2′-bipyridine). These electron acceptors, like the ruthenium complexes, bind to DNA noncovalently. For the phenanthroline series, intercalation and surface binding are possible, although Co(bpy)$_3^{3+}$ binds only electrostatically to the helix. The quenching mechanism with these donor-acceptor pairs is predominantly electron transfer. Evidence for electron transfer is supported by flash photolysis experiments. In addition, no Ru(phen)$_3^{2+}$-sensitized emission was observed from Cr(phen)$_3^{3+}$ or Rh(phen)$_3^{3+}$. Typical ruthenium concentrations used were 4 to 8 μ*M*, with ruthenium to nucleotide ratios ranging from 0.003 to 0.010, and acceptor concentrations varying from 0 to 80 μ*M*. Excited state lifetimes for both intercalative and surface-bound ruthenium were measured by deconvolution of the biexponential emission decay traces, and the rate constants were calculated for each component with the Stern-Volmer equation, $\tau_0/\tau = 1 + k_q\tau_0[Q]$, where τ is the lifetime of the luminescent species at quencher concentration [Q], τ_0 is the lifetime in the absence of quencher, and k_q is the bimolecular rate constant for quenching by photoinduced electron transfer (*13*). Since binding modes for the electron acceptors are not distinguished in this experiment, the analysis treats the acceptors as a single bound form.

Results of several quenching experiments with cobalt complexes as acceptors are summarized in Table 1. The electron-transfer rate constant from the surface-bound donor, k_q^s, is larger than k_q^i, the rate constant for electron transfer from the intercalatively bound species, for both Δ-Ru(phen)$_3^{2+}$ and Λ-Ru(phen)$_3^{2+}$. Small increases in the rate are apparent with Co(bpy)$_3^{3+}$, the nonintercalating and most weakly bound acceptor, in contrast to Co(phen)$_3^{3+}$. These results all point to a greater electron-transfer efficiency through surface rather than intercalative binding. In all cases, the rate constants for Λ-Ru(phen)$_3^{2+}$ are from 1.5 to 2 times greater than for Δ-Ru(phen)$_3^{2+}$, indicating enantiomeric selectivity. This observed stereoselectivity in electron-transfer rate constants is in contrast with the relative binding affinities of the complexes for DNA; phenanthroline complexes bind with greater affinity than bipyridyl complexes, and for Ru(phen)$_3^{2+}$, overall binding of the Δ-isomer is preferred. Enantiomeric selectivities for electron transfer that we observed differ from those reported previously, in which the donor-DNA ratio was much greater (1:30) (*8*). At the higher concentration ratios, the observed rate constants were governed largely by the local concentrations of donors and acceptors on DNA, and hence by relative binding strength. At low metal-DNA concentration ratios, nearly all of the donor molecules were bound, and the enhancements in electron-transfer rates, which are commensurately smaller, were not due to the effect of increased local concentrations. The observed stereoselectivity reflects fundamental differences in mechanisms for the electron transfer on DNA for the intercalated and surface-bound species, as well as their relative bound concentrations.

The fundamental differences between electron transfer from surface-bound and intercalated donors is even more dramatic upon examination of the temperature dependence of k_q^s and k_q^i with Δ-Ru(phen)$_3^{2+}$ as donor and Co(phen)$_3^{3+}$ as acceptor bound to DNA. The temperature dependence for these two cases is shown in Fig. 2. The surface-bound and intercalated Ru(phen)$_3^{2+*}$ behave quite differently with respect to electron transfer. The value of k_q^i increased little with temperature from 274 to 308 K. There was little variation in the value of k_q^s between 274 and 298 K, but above 298 K the quenching rate constant increased rapidly with increasing temperature. No change in DNA conformational state over this temperature range was detected by circular dichroism (CD). An Arrhenius plot of the data yields $\Delta H^{\ddagger}$ of ~2 kcal/mole for the intercalative electron transfer, and ~1 kcal/mole and ~16 kcal/mole for the two temperature regimes in the surface-bound case. Most simply, Fig. 2 provides verification of our model for intercalative and surface binding of tris(phenanthroline) metal complexes

Table 1. Electron-transfer rate constants (M^{-1} s^{-1}) from Δ- and Λ-Ru(phen)$_3^{2+}$ to *rac*-CoL$_3^{3+}$(L = phen, bpy). The driving force for the excited-state electron-transfer quenching reaction is approximately +1.29 and +1.24 V with Co(phen)$_3^{3+}$ and Co(bpy)$_3^{3+}$ as quenchers, respectively (*20*). Samples were 4 μ*M* Ru(phen)$_3^{2+}$ and 1.2 m*M* calf thymus DNA in 50 m*M* NaCl and 5 m*M* tris buffer (*p*H 7.2). Lifetime measurements were made with a PRA single photon counting unit that used a Model 510 nitrogen-filled nanosecond flash lamp with a pulsewidth of 3 ns and interfaced with a Digital RX02 minicomputer. Excitation and emission wavelengths were at 447 and 600 nm, respectively. Data were deconvoluted with a PRA data analysis package. The rate constants k_q^s, k_q^i, and k_q^c are for the surface-bound and intercalated donor on DNA, and free donor in solution, respectively. The average errors in rate constants are approximately ±20%. The control data were obtained with *rac*-Ru(phen)$_3^{2+}$ donor in the absence of DNA.

Donor	Acceptor					
	rac-Co(phen)$_3^{3+}$			*rac*-Co(bpy)$_3^{3+}$		
	k_q^s	k_q^i	k_q^c	k_q^s	k_q^i	k_q^c
Δ-Ru(phen)$_3^{2+}$	1.7×10^{10}	9.0×10^9	1.4×10^9	2.4×10^{10}	1.2×10^{10}	2.0×10^9
Λ-Ru(phen)$_3^{2+}$	3.9×10^{10}	1.6×10^{10}	1.4×10^9	4.7×10^{10}	1.7×10^{10}	2.0×10^9

to DNA, and also indicates that at least two distinct mechanisms for DNA-mediated electron transfer between bound metal complexes must operate.

In order to minimize collisional pathways for electron transfer, and thus distinguish between diffusion and long-range electron-transfer mechanisms, we also used high-viscosity glycerol solutions in a series of quenching experiments. The CD spectra of DNA solutions at these glycerol concentrations indicated no gross change in conformation from the B-form (*14*). At low temperature ($T < 273$ K), these solutions are sufficiently rigid to significantly reduce molecular transport (*15*). The local viscosity around the metal complexes when bound to DNA might be different from the bulk viscosity. However, a significantly lowered viscosity relative to the bulk would be required over many solvent layers, because of the diameters of the metal complexes themselves, to permit diffusion. Moreover, binding to DNA appears in itself to diminish the mobility of the complex, rather than increasing its mobility, as would be required for a diffusion mechanism. For example, the steady-state luminescence polarization for $Ru(phen)_3^{2+}$ in 90% glycerol solution at 293 K is increased from 0.001 to 0.103 (both values ±0.002 SEM) in the presence of DNA; the limiting polarization for $Ru(phen)_3^{2+}$ in a solid matrix is 0.14 (*16*). With decreasing temperature, still greater decreases in the mobility of the bound complex would be expected. Quenching results for ruthenium-cobalt pairs in glycerol solutions are summarized in Table 2. The rate for intercalated donors decreases by a factor of 5 upon the addition of glycerol, and no further with increasing viscosity. The value of k_q^s remains constant at $\sim 2 \times 10^{10} M^{-1}$ s^{-1}, even in the highest viscosity regime at low temperature. With $Co(bpy)_3^{3+}$ as a surface-bound acceptor, no decrease in surface-bound rate was apparent even at high glycerol concentrations and low temperature. Thus, under conditions where diffusion is restricted, DNA-mediated electron transfer remained enhanced compared with rates in the absence of DNA. For the surface-bound donor, in particular, the rate constant was two orders of magnitude greater compared with solution rates, and this enhancement could be increased even further if higher donor-DNA ratios were used.

That DNA accelerates electron transfer between bound metal complexes under conditions of substantially restricted mobility is illustrated further in Fig. 3, in which the quenching of $Ru(phen)_3^{2+*}$ by $Co(phen)_3^{3+}$ is plotted for the surface-bound component, the intercalated component, and for DNA-free solutions, in 92% glycerol at 253 K. The linearity of the plots supports the notion that the complexes are randomly distributed along the strand with no sequestering or cooperative association of the complexes on the polymer (*17*). In this essentially rigid system with low concentrations of donors and acceptors on the DNA (at these concentrations, the average separation between metal centers is in the range of 15 to 35 Å), surface-bound and, to a lesser extent, intercalated $Ru(phen)_3^{2+*}$ continue to transfer electrons to bound $Co(phen)_3^{3+}$, indicating that DNA promotes long-distance electron transfer between bound donors and acceptors. In the absence of DNA, the rate drops to below $10^7 M^{-1}$ s^{-1}, too low to be measured satisfactorily with this technique.

The logarithm of the decay trace for emission from the ruthenium excited state in the absence of DNA, in the presence of DNA, and with DNA and 32 μ*M* $Cr(phen)_3^{3+}$ at 253 K in glycerol solution is shown in Fig. 4. As for higher temperature experiments, in the absence of DNA a single exponential decay was observed. Upon addition of DNA, a biexponential decay was apparent, consistent with the two binding modes, and with the addition of $Cr(phen)_3^{3+}$, quenching by electron transfer was observed for the two components. The shorter lived surface-bound component was quenched appreciably faster than the long-lived component. Since the metal complexes, although fixed on the strand, are separated by a range of

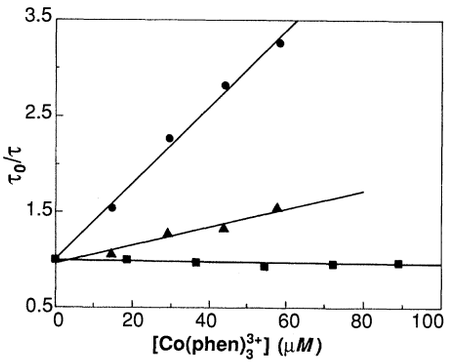

Fig. 3. Stern-Volmer plot of *rac*-$Ru(phen)_3^{2+}$ quenching by *rac*-$Co(phen)_3^{3+}$ in rigid glycerol solution (92% glycerol) at 253 K. Measurements were done with 4 μ*M* of $Ru(phen)_3^{2+}$ and 400 μ*M* of calf thymus DNA (●, surface, and ▲, intercalated), with the DNA excluded in the control experiments (■). Lifetime measurements were done in triplicate.

nearest-neighbor distances, the simple biexponential decays in emission were somewhat unexpected. The well-behaved binding isotherms, the absence of ruthenium self-quenching, and the high positive charges on both donors and acceptors all indicate that there was no clustering of metal complexes at the closest possible separation distance (4 base pairs), and thus a very shortlived component in emission corresponding to the particular contribution of donor acceptor reactions at the very closest distance was not observed. However, if the distribution of nearest-neighbor distances of donors and acceptors is broad (even for one type of donor), as occurs in a random distribution of donors and acceptors fixed in three-dimensional space, one might still expect a nonexponential decay in emission from the donor species (*18*). We determined the probability distribution for donors and acceptors fixed in one dimension along the DNA lattice (*19*) based upon equilibrium binding isotherms, previously obtained (*10*), which showed the metal complexes to be randomly distributed over 4-base-pair sites. Using this probability distribution of acceptor distances, we then calculated the expected sum of exponential decays in donor emission expected. We found that this sum of exponentials may be reasonably approximated by a single exponential in emission using the mean nearest-neighbor separation. Calculated decay traces based upon our probability distribution showed only a slight deviation from a single exponential, a deviation too small to be detected experimentally. Moreover, the best line fit through these calculated traces yielded donor lifetimes within 10% of experimental value. The good fit and close approximation of the sum of exponentials to a single exponential decay

Table 2. Electron-transfer rate constants in viscous media. Solutions were 4 μ*M* $Ru(phen)_3^{2+}$ and 400 μ*M* calf thymus DNA for measurement of k_q^s and k_q^i, and with no DNA for k_q^c. Average errors in the ratio constants are approximately 20%.

Acceptor	Conditions			Rate constants		
	Glycerol content (%)	Temperature (K)	η (cP)	$k_q^s \times 10^{10}$ (M^{-1} s^{-1})	$k_q^i \times 10^{10}$ (M^{-1} s^{-1})	$k_q^c \times 10^{10}$ (M^{-1} s^{-1})
$Co(phen)_3^{3+}$	0*	274	1.8	1.7	0.9	0.15
$Co(phen)_3^{3+}$	60	274	25	1.6	0.2	0.03
$Co(phen)_3^{3+}$	84	274	349	1.8	0.2	0.04
$Co(bpy)_3^{3+}$	84	274	349	2.4	0.2	0.02
$Co(phen)_3^{3+}$	92	253	12,163	2.4	0.2	(<0.001)†

*Data from Δ-$Ru(phen)_3^{2+}$ donor. †Too low to be measured by SPC lifetime quenching.

may be a function both of the fact that the distribution is over a one-dimensional lattice (with a reduced number of nearest neighbors compared with that in multidimensional space) and the fact that there may be a weak dependence of rate on distance.

The application of transition metal complexes to these electron-transfer studies makes varying the thermodynamic driving force and examining the effect of such variation on the electron-transfer rate convenient. If reactions between the metal complexes were diffusion limited, then little sensitivity in electron-transfer rate to free energy change between donor and acceptor would be expected. Table 3 shows electron-transfer rates for photoinduced electron transfer from $Ru(phen)_3^{2+*}$ to phenanthroline complexes of Rh, Cr, and Co in the presence of DNA in glycerol solutions at 293 and 253 K. In the absence of DNA at 298 K, with $Ru(phen)_3^{2+*}$ as donor and the acceptors $Rh(phen)_3^{3+}$, $Cr(phen)_3^{3+}$, and $Co(phen)_3^{3+}$, ΔE^0 is estimated to be 0.22, 0.64, and 1.29 V, respectively (*20*). In accord with Marcus theory, for this range of driving forces in the absence of DNA, the electron-transfer rate constants increase with increasing driving force (*21*). In the presence of DNA, however, the rate constants vary substantially with driving force and not as expected. The ratios of rate constants in the presence of DNA to the absence of DNA at 293 K with a surface-bound Ru donor and Cr or Rh acceptor are ~250 and ~50, respectively. At 253 K in rigid medium, for the series of acceptors $Co(phen)_3^{3+}$, $Cr(phen)_3^{3+}$, and $Rh(phen)_3^{3+}$, the electron-transfer rate constants with surface-bound $Ru(phen)_3^{2+*}$ are 2.4×10^{10}, 5.0×10^{10}, and $0.14 \times 10^{10} M^{-1}\ s^{-1}$, respectively. For intercalated $Ru(phen)_3^{2+*}$, enhancements vary similarly. This variation in enhancement for the series of metal complexes indicates that the accelerated rates on DNA cannot be a local concentration effect. The different $M(phen)_3^{3+}$ complexes bind equally well to DNA. Furthermore, DNA-facilitated diffusion cannot account for the enhancements, since the greatest change should be seen for the diffusion-limited Co acceptor, with relatively reduced enhancements for those reactions of lesser driving force. These variations in rate constant with free energy based upon a simple adiabatic reaction between the metal complexes are difficult to interpret with Marcus theory based on solvent reorganization energies for systems free in solution. Binding to DNA may alter these reorganization energies. In addition, the large rate enhancements seem to require that the DNA serves as an intervening medium, one which facilitates the electron transfer (*22*). The remarkable rate enhancement evident with $Cr(phen)_3^{3+}$ as acceptor may indicate a particularly close matching of the electronic states of DNA coupling the excited donor to the Cr complex.

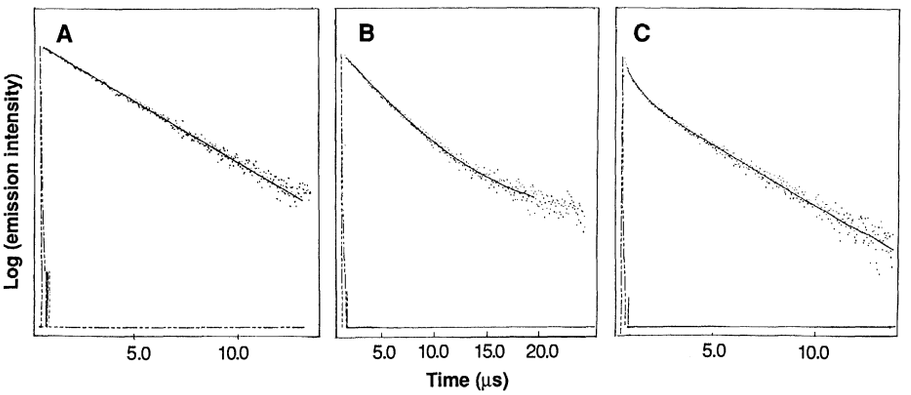

Fig. 4. Logarithmic decay traces obtained by single-photon counting for emission from $Ru(phen)_3^{2+*}$ at 253 K in 90% glycerol (**A**) in the absence of DNA, (**B**) in the presence of 600 μ*M* DNA and 4 μ*M* $Ru(phen)_3^{2+}$, and (**C**) with 480 μ*M* DNA and 32 μ*M* $Cr(phen)_3^{3+}$.

Table 3. Electron-transfer rate constants with $Ru(phen)_3^{2+*}$ as donor, illustrating variations with thermodynamic driving force. For an explanation of the determination of ΔE^0 in the absence of DNA, see (*20*). Average errors are approximately 20%. Solutions with DNA contained 4 μ*M* $Ru(phen)_3^{2+}$ and 600 μ*M* calf thymus DNA.

Acceptor	Temperature (K)	ΔE^0 (V)	Rate constants ($M^{-1}\ s^{-1}$)		
			$k_q^c \times 10^{10}$	$k_q^s \times 10^{10}$	$k_q^i \times 10^{10}$
		No DNA or glycerol			
$Co(phen)_3^{3+}$	293	1.29	0.14		
$Cr(phen)_3^{3+}$	293	0.64	0.05		
$Rh(phen)_3^{3+}$	293	0.22	0.02		
		DNA and 90% glycerol			
$Cr(phen)_3^{3+}$	293			11.7	0.96
$Rh(phen)_3^{3+}$	293			0.8	0.17
$Co(phen)_3^{3+}$	253		<0.001*	2.4	0.2
$Cr(phen)_3^{3+}$	253			5.0	0.64
$Rh(phen)_3^{3+}$	253			0.14	0.086

*Too low to be measured by SPC lifetime quenching.

Enhancements in diffusion-limited reaction rates for processes that occur on macromolecules have been reasonably attributed to enhanced diffusion of the reactants along the macromolecular surface (*23*). In several systems involving DNA-binding proteins, reductions in the dimensionality of space in which the reaction occurs can increase the rate by several orders of magnitude (*24, 25*). We initially thought that such one-dimensional diffusion along the DNA would also account primarily for the enhancements in DNA-mediated quenching rate between bound donor-acceptor pairs, as described here. Such a mechanism for slipping along the strand may serve, at least in part, to enhance the rates of DNA-bound electron transfer at higher temperatures.

Experiments in rigid solution and with variations in driving force, however, point to another mechanism for DNA-mediated electron transfers. The persistence of enhanced reaction rates upon binding to DNA under conditions sufficient to minimize the translational motion of the bound species indicates that long-range electron transfer may proceed through the DNA. Surprisingly, the more mobile surface-bound ruthenium complex appears to promote long-range transfer with greater efficiency than the intercalated species, despite the proximity of the latter to the extensive π framework of the stacked bases. This difference in electron transfer for the two bound forms may result in part from the differing orientations of the bound species on the DNA strand. Additionally, the results suggest that the sugar-phosphate backbone may play a significant role in electron transport (*26*). The solvent medium, oriented by the DNA polyanion, may provide a particularly low barrier for tunneling (*27*). The strong electronic coupling may also be a consequence of the accessibility of low-lying excited states on the DNA. The sensitivity of the rate to thermodynamic driving force supports this notion. Thus the efficiency of electron transfer depends upon binding mode, that is, orientation of donor and acceptor on the polymer, as well as upon the electronic states

of donor and acceptor, and how well these electronic states couple with the intervening DNA. It is not clear that nature has taken advantage of the DNA polymer as a mediator of electron transfer, but in fact oligonucleotides and polynucleotides should serve well as vehicles that may be readily manipulated to examine systematically the effects of medium, orientation, and separation distance on electron transfer in a polymeric system.

REFERENCES AND NOTES

1. D. Devault, *Q. Rev. Biophys.* **13**, 387 (1980).
2. S. L. Mayo, W. R. Ellis, R. J. Crutchley, H. B. Gray, *Science* **233**, 948 (1986); S. S. Isied, *Prog. Inorg. Chem.* **32**, 443 (1984).
3. J. L. McGourty, W. V. Blough, B. M. Hoffman, *J. Am. Chem. Soc.* **105**, 4472 (1983); N. Liang, C. H. Kang, P. S. Ho, E. Margoliash, B. M. Hoffman, *ibid.* **108**, 4665 (1986); K. P. Simolo, G. L. McLendon, M. R. Mauk, A. G. Mauk, *ibid.* **106**, 5012 (1984); G. L. McLendon and J. R. Miller, *ibid.* **107**, 7811 (1985).
4. J. J. Hopfield, *Proc. Natl. Acad. Sci. U.S.A.* **71**, 3640 (1974); M. Redi and J. J. Hopfield, *J. Chem. Phys.* **72**, 6651 (1980).
5. R. A. Marcus, *Annu. Rev. Phys. Chem.* **15**, 155 (1964); *J. Phys. Chem.* **72**, 891 (1968); R. A. Marcus and N. Sutin, *Biochim. Biophys. Acta* **811**, 265 (1985).
6. G. L. Closs, L. T. Calcaterra, N. J. Green, K. W. Penfield, J. R. Miller, *J. Phys. Chem.* **90**, 3673 (1986).
7. A. D. Joran, B. A. Leland, G. G. Geller, J. J. Hopfield, P. B. Dervan, *J. Am. Chem. Soc.* **106**, 6090 (1984); A. D. Joran *et al.*, *Nature* **327**, 508 (1986).
8. J. K. Barton, C. V. Kumar, N. J. Turro, *J. Am. Chem. Soc.* **108**, 6391 (1986).
9. P. Fromherz and B. Rieger, *ibid.*, p. 5361.
10. J. K. Barton, A. T. Danishefsky, J. M. Goldberg, *ibid.* **106**, 2172 (1984).
11. C. V. Kumar, J. K. Barton, N. J. Turro, *ibid.* **107**, 5518 (1985); J. K. Barton, J. M. Goldberg, C. V. Kumar, N. J. Turro, *ibid.* **108**, 2081 (1986); J. Rehmann, thesis, Columbia University, New York (1988).
12. J. K. Barton, *Science* **233**, 727 (1986).
13. N. J. Turro, *Modern Molecular Photochemistry* (Benjamin-Cummings, Menlo Park, CA, 1978), p. 246.
14. R. B. Macgregor, R. M. Clegg, T. M. Jovin, *Biochemistry* **26**, 4008 (1987); V. I. Ivanov, L. E. Minchenkova, A. Schyolkina, A. I. Poletayev, *Biopolymers* **12**, 89 (1973). The ratio of intercalation to surface binding of $Ru(phen)_3^{2+}$ does increase appreciably with glycerol present in solution. Thus it is likely that $Co(phen)_3^{3+}$ exists also predominantly in the intercalated form under these conditions.
15. T. Guarr, M. Mcguire, S. Strauch, G. McLendon, *J. Am. Chem. Soc.* **105**, 616 (1983). Under these conditions, the bulk viscosity is estimated to be 1.2×10^4 cP, and the calculated diffusion distance for the metal complexes not bound to DNA would be approximately 4 Å during the lifetime of the donor excited state.
16. I. Fujita and H. Kobayashi, *Inorg. Chem.* **12**, 2758 (1973).
17. The absence of self-quenching of the ruthenium excited state further supports this assumption.
18. M. Inokuti and F. Hirayama, *J. Chem. Phys.* **43**, 1978 (1965).
19. The distribution of separation distances was calculated with the nearest-neighbor distance distribution for a "hard rod gas" distributed randomly over a one-dimensional lattice

$$P(r)dr = \frac{N}{[L(1 - N\sigma/L)]} \times \left[1 - \frac{(r - \sigma)}{[L(1 - N\sigma/L)]}\right]^{N-1} dr,\ r \geq \sigma$$

where N is the number of bound particles with an exclusion length σ bound to a lattice of length L. In our case, L is 200 base pairs, σ is 4 base pairs per bound molecule, and N is the sum of donor and acceptors. The mean distance, $\langle r \rangle$, is

$$\langle r \rangle = \Sigma rP(r)/\Sigma P(r)$$

See L. Tonks, *Phys. Rev.* **50**, 955 (1936).
20. Driving forces were calculated based upon data reported in the following references: B. Brunschwig and N. Sutin, *J. Am. Chem. Soc.* **100**, 7568 (1978); S.-F. Chen *et al.*, *ibid.* **103**, 369 (1981); E. Paglia and C. Sironi, *Gazz. Chim. Ital.* **87**, 1125 (1957).
21. In buffer at 293 K in the absence of DNA, the rates with either Cr or Co as acceptor appear to be diffusion controlled based upon measurements at different ionic strengths, whereas the reaction with Rh, having a substantially smaller free energy change, is activation limited.
22. Results that vary in this fashion with driving force may be interpreted in terms of donor-acceptor pairs in the Marcus inverted region. For these experiments, however, the DNA would still be involved in mediating such transfer. In a model system, the possible role of virtual states of an intervening π-electron system has been discussed. See H. Heitele and M. E. Michel-Beyerle, *J. Am. Chem. Soc.* **107**, 8286 (1985).
23. G. Adams and M. Delbruck, in *Structural Chemistry and Molecular Biology*, A. Rich and N. Davidson, Eds. (Freeman, San Francisco, 1968), p. 198; P. Richter and M. Eigen, *Biophys. Chem.* **2**, 255 (1974).
24. O. G. Berg, R. B. Winter, P. H. von Hippel, *Biochemistry* **20**, 6929 (1981).
25. B. J. Terry, W. E. Jack, P. Modrich, *J. Biol. Chem.* **260**, 13130 (1985).
26. Theoretical studies have actually noted that some charge transfer from the ribose units along the DNA backbone to the bases may occur, creating what is essentially a substantial hole framework on the DNA backbone. See P. Otto, E. Clementi, and J. Ladik [*J. Chem. Phys.* **78**, 454 (1983)] and E. Clementi and G. Corongiu [*Int. J. Quant. Chem. Quant. Biol. Symp.* **9**, 213 (1982)].
27. Replacing the NaCl in our buffer with 30 m*M* $MgCl_2$, which may perturb the solvent structure around the helix, causes a decrease for k_q^s to $7 \times 10^9 M^{-1}\ s^{-1}$, with k_q^i remaining constant.

28. We thank B. Berne for stimulating discussions regarding the near-neighbor distance distributions. Supported by National Science Foundation and the Army Office of Research.

14 April 1988; accepted 26 July 1988

Imaging of Phosphorescence: A Novel Method for Measuring Oxygen Distribution in Perfused Tissue

WILLIAM L. RUMSEY,* JANE M. VANDERKOOI, DAVID F. WILSON

The imaging of phosphorescence provides a method for monitoring oxygen distribution within the vascular system of intact tissues. Isolated rat livers were perfused through the portal vein with media containing palladium coproporphyrin, which phosphoresced and was used to image the liver at various perfusion rates. Because oxygen is a powerful quenching agent for phosphors, the transition from well-perfused liver to anoxia (no flow of oxygen) resulted in large increases of phosphorescence. During stepwise restoration of oxygen flow, the phosphorescence images showed marked heterogeneous patterns of tissue reoxygenation, which indicated that there were regional inequalities in oxygen delivery.

IN MAMMALIAN TISSUES, OXYGEN MUST be continuously supplied to maintain cellular homeostasis. Even moderate reductions of blood flow compromise physiological function. In order to investigate the nature of oxygen supply to tissue in detail, a method is needed for the accurate measurement of the concentration of oxygen at its site of transfer from the vascular bed to parenchymal cells. Methods that have been used to assess tissue oxygenation not only have individual technical problems but in general are weakened by their inflexibility. For example, oxygen microelectrodes are not always suitable because (i) they are restricted to specific locations within the tissue, thereby preventing evaluation of a large area, and (ii) they must be inserted into the tissue, which disturbs its local environment.

Recently we developed a method for measuring oxygen that is based on its ability to quench phosphorescence of selected luminophores (*1, 2*). This method is accurate and provides precise serial measurements of oxygen in the physiological range, from $10^{-3}M$ to less than $10^{-8}M$. To date, however, this methodology has been restricted to the in vitro study of biological samples that can be placed in a cuvette, such as suspensions of isolated mitochondria (*3*) and cells (*4*). We have shown that phosphorescence measurements can be used to obtain images of oxygen distribution in tissue without invasion of that tissue. Inhomogeneities of oxygen delivery to tissue of isolated perfused rat liver have been demonstrated with a video camera, which detects the phosphorescence of palladium (Pd)-coproporphyrin in the tissue perfusate.

When the tissue is illuminated, some light is absorbed by the Pd-coproporphyrin, which excites it to the triplet state. The

Department of Biochemistry and Biophysics, University of Pennsylvania School of Medicine, Philadelphia, PA 19104.

*To whom correspondence should be addressed.